IJE TRANSACTIONS B: Applications Vol. 28, No. 8, (August 2015) 1209-1218

International Journal of Engineering

Journal Homepage: www.ije.ir

Prediction of Residual Stresses for a Hollow Product in Cold Radial Forging Process

M. Poursina*[a], H. Alijani Renani[a], B. Ghasemi[b]

[a] *Department of Mechanical Engineering, University of Isfahan, Iran*
[b] *Department of Mechanical Engineering, Khomeini shahr Azad University, Iran*

PAPER INFO

Paper history:
Received 02 April 2015
Received in revised form 23 May 2015
Accepted 30 July 2015

Keywords:
Cold Radial Forging
Residual Stress
Mandrel Forging
3-D FEM.

ABSTRACT

Radial forging is an open die forging process used in reducing the diameters of shafts, tubes, stepped shafts and axles in addition to creating internal profiles such as rifling the gun barrels. The radial forging of tube is usually performed over a mandrel to create an internal profile and/or size the internal diameter. Most of the previous studies conducted on the radial forging process have used axisymmetric models. In this study, the residual stresses of a short hollow tube in a cold radial forging process is assessed through 3-D finite element simulation. The mandrel used here contains six helical grooves and two steps along its length. This kind of mandrel is innovated in this research. The workpiece is modeled as an elastic-plastic material and the commercial finite element software, ABAQUS is used to simulate the process. The accuracy of the finite element model is tested by comparing the predicted results with available experimental works and is validated by both the slab and upper bound methods. Residual stresses in the radial forged product and influence of the process parameters on stress distribution, such as workpiece motions, friction and percentage of reduction are studied to determine the optimized parameters of simulation and improve the condition of this process.

doi: *10.5829/idosi.ije.2015.28.08b.14*

NOMENCLATURE

m	Stick friction coefficient	**Greek Symbols**	
n	Material coefficient	β	Angel of cross section
K	Material coefficient	μ	Columb friction coefficient
Z	Axis along the mandrel	$\bar{\sigma}$	Mean flow stress (N/m^2)
		τ_f	Magnitude of friction shear stress
		τ_y	Magnitude of yield shear stress

1. INTRODUCTION

The surface condition of a product can be rated according to its surface quality, the latter being determined by properties such as surface roughness, hardness variation, structural change, and residual stress. Among these properties, the residual stress distribution is one of the primary aspects of surface quality because of its significant effect on the fatigue life, deformation and dimensional stability of the product [1]. A stress field on the surface of a product can lead to a crack, which could be propagated rapidly, but it can also squeeze a crack shot. If the surface stresses are tensile and tend to enlarge the crack, it contributes to the destruction of the part. In contrast, small cracks in a compressive stress field created by the corrosive or local deformation do not grow in a rapid manner as they would do normally [2].

Radial forging is a hot/cold forging process utilizing two or more radially moving anvils or hammer dies, to

*Corresponding Author's Email: *poursina@eng.ui.ac.ir* (M. Poursina)

Please cite this article as: M. Poursina, H. Alijani Renani, B. Ghasemi, Prediction of Residual Stresses for a Hollow Product in Cold Radial Forging Process, International Journal of Engineering (IJE), TRANSACTIONS B: Applications Vol. 28, No. 8, (August 2015) 1209-1218

produce solid or tubular components with varying cross section along their lengths. This process is usually applied in reducing the diameters of solid and hollow products, forging of stepped shafts and axles, forging of guns and rifle barrels, and producting tubular components with or without internal profiles. Alloys like steel alloys, titanium alloys, and metals like beryllium, tungsten, and high-temperature super-alloys are used in this process. The principle schematic of the radial forging of rods with a four-hammer radial forging machine is shown in Figure 1. Deformation results from short-strokes side-pressing operations which are performed usually by four forging tools, are arranged radially around the workpiece.

Radial forging process, RFP, is capabile of manufacturing of virtually chip-less rods and tubes to provide a product with almost 95% precision-finishing [3]. The properties of radially forged products include tight tolerances, smooth surface finish, preferred fiber structure, minimum notch effect, and homogeneous grains and this is due to a uniform effect of the process to the core of the workpiece [4]. In the RFP, deformation in the process results from a great number of short strokes and high-speed hammer blows on the workpiece. After each blow, the workpiece is rotated and axially fed toward the entrance of the dies; consequently, at each stroke only a small portion of the workpiece is subject to plastic deformation; hence a fairly low-load requirement. The simultaneous rotational motion and axial feed of the workpiece allows production to be in round pieces and internally-profiled tubes.

The deformation zones in tube radial forging are illustrated in Figure 2. Deformation in this process occurs in three distinctive zones: sinking, forging and sizing. In the sinking zone, both the inner and outer diameters of the tube are reduced. In the forging zone, the inner diameter of the tube is equal to the outer diameter of mandrel and only the outer diameter of the tube is reduced. In the sizing zone, both the inner and outer diameters of the tube have almost reached their final lengths and only a small amount of plastic deformation occurs in the tube.

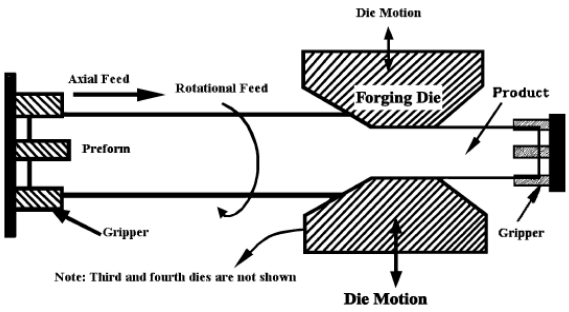

Figure 1. The principle of radial forging machines [3]

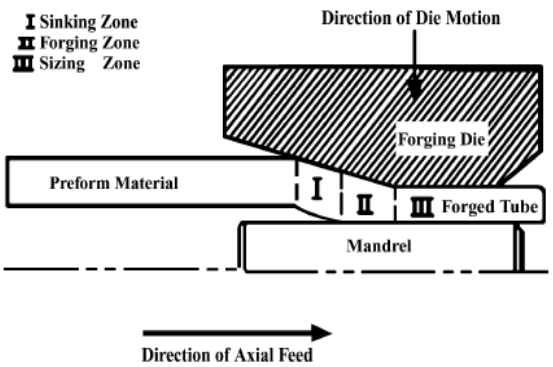

Figure 2. Deformation zones (sinking, forging and sizing) in tube radial forging process [3]

2. LITERATURE REVIEW

Radial forging was first developed in Austria in 1946. It was initially used for hot forging of small parts and cold forging of tubes over mandrels [3]. Lahoti et al. [4, 5] analyzed the mechanics of RFP for single and compound angle dies using the slab method. Domblesky et al. [6] presented a finite element model, FEM, to determine the strain, strain rate, and temperature distribution in radial forging. Jang and Liou [7] also modelled radial forging using the FEM to evaluate the residual stresses in symmetric products, by applying a modular upper bound technique. Subramanian et al. [8] modelled the metal flow in the die cavity in radial forging for rifling of the gun barrels under plane strain conditions. The objectives of their study were to investigate the metal flow in the rifling of the gun barrels and to determine the influence of process variables on metal flow. Yang [9] conducted a study on the RFP using the combination of slip-line theory with the upper bound method under plane strain conditions. He used the slip-line field and a hodograph coupled with the use of a non-linear optimization technique to find the field angles and other defining parameters. The results of his study indicates that this procedure provides a strong method for calculating the complicated slip-line field solutions. Ameli et al. [10], in a parametric study, investigated the residual stresses in a cold radial forging product by axisymmetric simulation of RFP on a four internal helical groove tube. Ghaei et al. [11] used the upper bound method to find the maximum required forging load in a RFP. In another work, Ghaei et al. [12] studied die design for the RFP. Mahmoudi et al. [13] used contour method to measure the residul stresses. They compared the results of contour method, which simulated by finite element analysis, with the experimental results.

In this proposal, the residual stresses of a tube with a complicated internal profile are studied through the 3D

simulation model. The tube used here contains six internal helical grooves and two steps along its length. Due to the lack of direct experimental data for verification of simulation and boundary condition, the results of the 3D FEM are validated by some experimental data for forging of cylindrical parts without internal profile introduced by Uhlig [14], the results of the slab method [4] and the results of the upper bound method [11]. There are two vital parameters affecting the fatigue life of the product. These important parameters are including pattern of residual stresses and stress concentrations around the tube internal profile. In this study, both mentioned parameters are taken into consideration. The effects of process parameters such as workpiece motions, axial and rotational feed, friction and the percentage of deformation on residual stresses are assessed as well.

3. FINITE ELEMENT MODELLING

The FEM should be able to analyze complex deformations for the determination of material flow. In this study, the commercial finite element code, ABAQUS/Explicit, is used to model the RFP and to determine residual stresses on the product. The RFP is characterized by complex cyclic and transient loading conditions.

The modeling strategy used in this study is to model the process on a stroke-by-stroke basis using a 3-D model. The workpiece is modeled as an elastic-plastic material with eight node continuum cube elements with reduced integration and hourglass control (C3D8R). Here the four node rigid rectangular elements (R3D4) are used for modeling the die and the rigid surfaces of the mandrel. The FEM is applied to simulate the forging process, is shown in Figure 3.

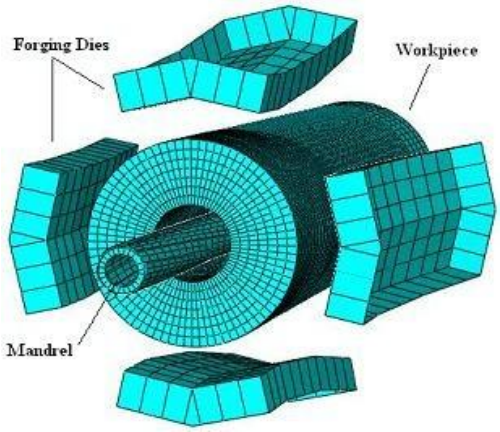

Figure 3. Cold radial forging FE Model

A combination of Coulomb law and constant limit shear is used to model the friction at the contact surfaces, where the limiting shear stress is obtained as $m\bar{\sigma}/\sqrt{3}$; where, $\bar{\sigma}$ is the flow stress and m=0.15 is the friction coefficient commonly used for cold forging conditions [4]. The Coulomb friction coefficient here is set at 0.2 [12, 15].

If the Columb friction law is only under taken, the magnitude of friction shear stress, τ_f, will be greater than the magnitude of yield shear stress, τ_y, due to the large magnitude of the radial forging force. Therefore, the combination of Columb friction law and stick friction, according to the Equation (1) is used in this study, where $\bar{\sigma}$ is the mean flow stress, $\mu$is the Columb friction coefficient and m is the stick friction coefficient.

$$\tau_f = \begin{cases} \mu\sigma_N & if \quad \tau \le \tau_y \\ m\bar{\sigma}/\sqrt{3} & if \quad \tau \rangle \tau_y \end{cases} \quad (1)$$

In this study, the effects of strain rate and temperature are neglected because the heat generated in the process is not high enough to change the material or process parameters significantly; therefore, the process may be assumed as isothermal. That is the heat generated during plastic deformation offsets the heat dissipation by cooling. Since the process is assumed to be a cold forging, a power law for strain hardening is used as follows:

$$\sigma = K\varepsilon^n \quad (2)$$

The workpiece material is of AISI 1015. The K and n values in room temperature are provided by [16]:

K=618.14 MPa, n=0.1184.

The properties of workpiece material are tabulated in Table 1.

The radial velocity of each die is subjected to a harmonic or sinusoidal function like the slider crank mechanism. This process is simulated in one pass of 40 strokes. The dimensions of the workpiece and the hammers used in modelling of cold RFP are tabulated in Table 2.

TABLE 1. Elastic-plstic properties of material

Properties	Value
Elasticity modulus (Pa)	200e9
Density (kg/m^3)	7850
Yield stress (Pa)	205e6
Poison ratio	0.28

TABLE 2. Geometry of workpiece and hammer in cold RF

Title	Dimension
Length of workpiece	100 mm
Outer diameter of preform	27.5 mm
Inner diameter of preform	10.3 mm
Outer diameter of product	22 mm
Inner diameter of product	5.56 mm
Reduction in area	31%
Die land length	10 mm
1st die inlet angle	6°
2nd die inlet angle	9.5°
1st die inlet length	21 mm
2nd die inlet length	24 mm
Total length of die	70 mm
Maximum velocity of die per stroke	12 mm/s
Axial feed per stroke	0.9 mm
Rotational feed per stroke	15°
Angular Velocity	33.33 RPM

The 2D and 3D geometry of compound dies, used in RFP analysis are illustrated in Figures 4 and 5. In the die throat length, usually two flat surfaces meet an angle. This angle between the two intersecting surfaces is constant and is equal to 155°.

The purpose of using the mandrel during forging is to prevent collapse of the inner wall of the tube and to form the inner wall diameter. Depending on the internal profile to be produced, there are two basic types of mandrels applied in radial forging: the "short" and "long" mandrels. Short mandrels are used in the forging of the long tubes where the inner diameter is constant along the length of the workpiece.

Figure 4. 2D view of die land and die inlets of hammer in RFP

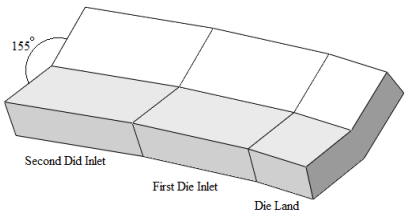

Figure 5. 3D view of die land and die inlets of hammer in RFP

Long mandrels are used for forging short tubes where the inner diameter is stepped along the length of the workpiece. For stepped tubes, the mandrel moves simultaneously with the workpiece through the forging box [6]. The mandrel used in this study is a caliber 5.56, of the long type with a cartridge chamber with two steps, and six grooves that are swept helically along the axial direction with a pitch of 304.8 mm. The dimensions of the mandrel used in modeling of cold RFP are tabulated in Table 3.

The cross-sectional view of the mandrel in the grooves area used in this 3-D simulation is shown in Figure 6.

The schematic 3D view of the same mandrel is shown in Figure 7.

Some researchers have simulated the nodes at the end of the workpiece as fixed in the axial direction in RFP[5].

TABLE 3. Geometry of mandrel used in cold radial forging

Title	Dimension
Larg diameter of mandrel (D)	6 mm
Small diameter of mandrel (d)	5.56 mm
1st mandrel step angle	22.8°
2 nd mandrel step angle	22.8°
Mandrel taper	0.05mm for a length of 60 mm
Total length of mandrel	130 mm

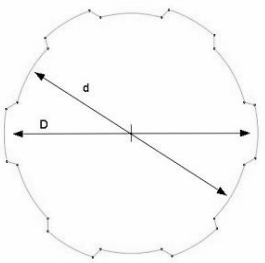

Figure 6. Cross-sectional of mandrel

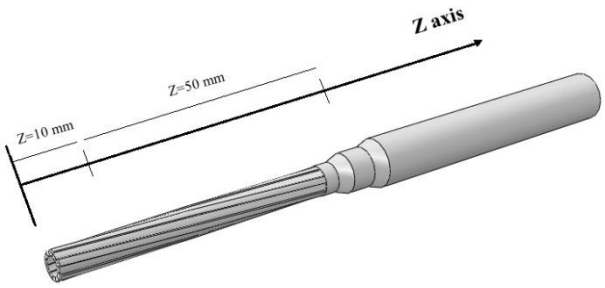

Figure 7. The schematic view of the mandrel

In reality, there are several sets of springs in the chuck- head which allow limited movement of the workpiece in the axial direction during the process and this factor is applied in the simulation. These restrains have a great influence on the metal flow; That is, the impact of hammers on the workpiece compress the springs and prior to other impacts these springs produce a backward force on the workpiece. This backward movement increases the total radial forging load and promotes the material flow in the forward direction [17].

4. VALIDATION OF SIMULATION

It is essential to validate the numerical model prior to presenting the simulation results. As mentioned, there exists no direct experimental data related to this assessment. Therefore, the results of this 3D FEM are validated through some experimental data for forging the cylindrical parts without internal profile introduced by Uhlig [12]. The validation of the cold RFP modeling is obtained for four different cases by applying the experimental measurements, the slab method, as well as the upper bound method predictions.

For this purpose, finite element simulations of radial cold forging of AISI 1015 steel billet with a friction coefficient of 0.15, inlet angle of 4.3°, axial feed per stroke of 0.37 mm, length of the sizing zone of 18 mm and length of the forging zone for these four diffrent cases 18.55 mm, 18.09 mm, 12.77 mm and 6.38 mm is carried out. The dimensions of the primary and secondary diameter of the workpiece used in this four simulation cases are presented in Table 4.

The comparisons between calculated RFP load, according to FEM, and other methods are made and expressed in Table 5. As observed in Table 5, there is a good agreement between the FEM results and the experimental measurements, the slab method, as well as the upper bound method predictions. As expected, the upper bound method has the maximum values, for the four cases studies.

TABLE 4. Diameters of workpiece and die in cold RF

Title	Dimension
Outer diameter of workpiece in case 1	15.97mm
Outer diameter of product in case 1	13.18mm
Outer diameter of workpiece in case 2	15.97mm
Outer diameter of product in case 2	13.25mm
Outer diameter of workpiece in case 3	15.03mm
Outer diameter of product in case 3	13.11mm
Outer diameter of workpiece in case 4	13.99mm
Outer diameter of product in case 4	13.03mm

TABLE 5. Comparison between FEM maximum predicted loads and the results obtained from the other methods [KN]

Case No.	Slab Method [4]	Upper Bound [11]	Experimental [14]	FEM	Error (%)
1	171.98	193.22	172	180.6	4.7
2	170.62	190.42	167	178.4	6.4
3	143.37	149.79	124	128.8	3.7
4	106.18	105.79	74.5	79.8	6.6

Errors are calculated according to the magnitudes of FEM and the experimental results. These magnitude of errors is a very common in the engineering problems and are acceptable. Therefore, the numerical simulation and its boundary conditions, are modelled well and are in a good agreement with other results obtained so far. Consequently, the developed FEM can be used in other aspects of radial forging process like residual stresses [9].

5. RESULTS AND DISCUSSION

The residual stresses distributions in the radial forged product and effects of various process parameters like the workpiece motions, friction and percentage of reduction on the distribution of the residual stresses of the product are discussed. The cross-sectional view of a tube where angle β is defined is shown in Figure 8.

The results are mentioned in two cross sections, z=10mm which is located athelical grooves, and z=50mm, which is located between two steps of themandrel (Figure 7).

The distribution of axial, shear, hoop and radial residual stresses at the cross-section of z=10 mm (measured from the tip of the workpiece in the axial direction) on the inner and outer surface of the workpiece where helical grooves are located are shown in Figures 9 to 12.

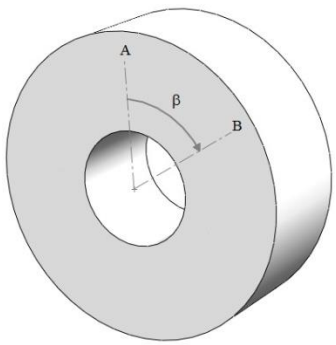

Figure 8. The cross-sectional view of a tube

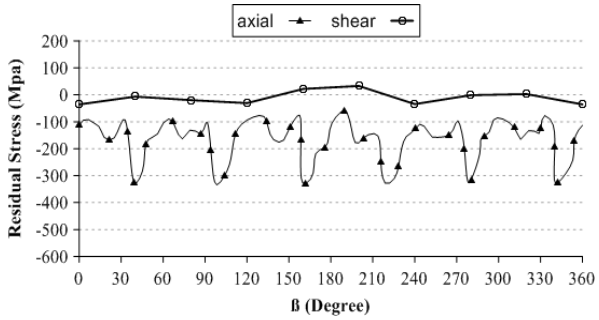

Figure 9. Axial and shear residual stresses in the cross-section of z=10 mm on the inner surface

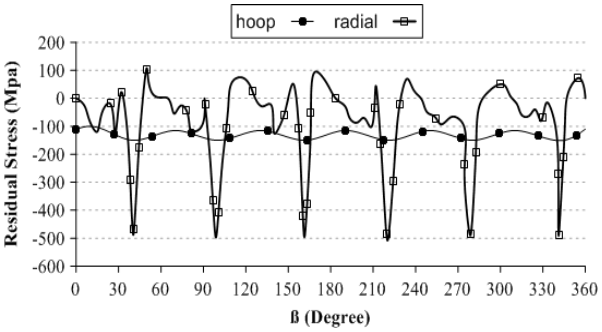

Figure 10. Hoop and radial residual stresses in the cross-section of z=10 mm on the inner surface

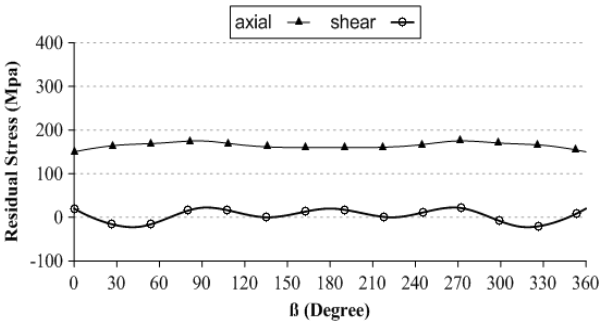

Figure 11. Axial and shear residual stresses in the cross-section of z=10 mm on the outer surface

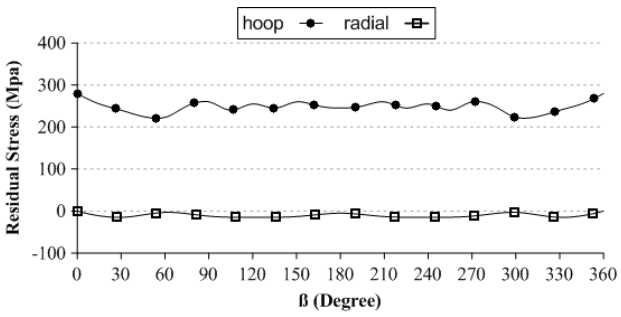

Figure 12. Hoop and radial residual stresses in the cross-section of z=10 mm on the outer surface

As shown in Figures 9 and 11, the shear residual stress on the both surfaces is small and negligible, indicating that this problem is symmetric, that is, the axial, radial, and hoop directions constitute the principle stress axis. Indeed, the small but nonzero nodal stresses obtained from FE are generated due to stresses obtained at the integration points of the elements which are averaged at nodal points on the surface [7, 10].

The residual stresses on the inner surface are mostly compressive and can enhance the prevention of crack propagation. Since such products usually operate under high internal pressures, compressive residual stresses on the inner surface can improve product life. Due to existence of six helical grooves on the inner surface of the tube, the axial and radial residual stresses have six compressive peaks in the stress profile.

In the outer surface, the axial and hoop residual stresses are tensile, thus it may promote the propagation of possible cracks to a point that it may need to be stress relieved before use. Because hammers are removed and there is no stress concentration on the outer surface, these surfaces are free and the radial stress is removed.

The profile of axial, shear, hoop and radial residual stresses in the cross-section of z=50 mm on the inner and outer surface of the workpiece between two steps are shown in Figures 13 to 16.

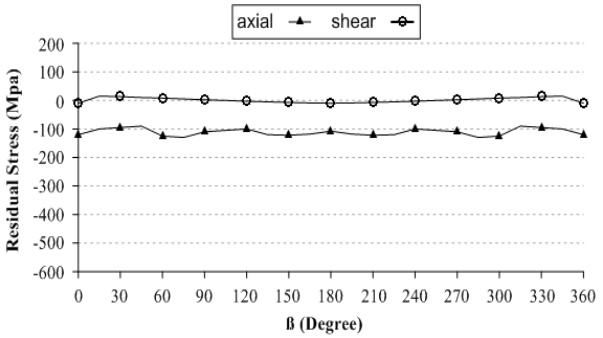

Figure 13. Axial and shear residual stresses in the cross-section of z=50 mm on the inner surface

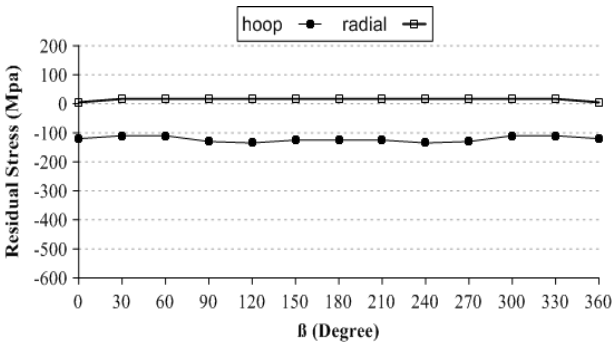

Figure 14. Hoop and radial residual stresses in the cross-section of z=50 mm on the inner surface

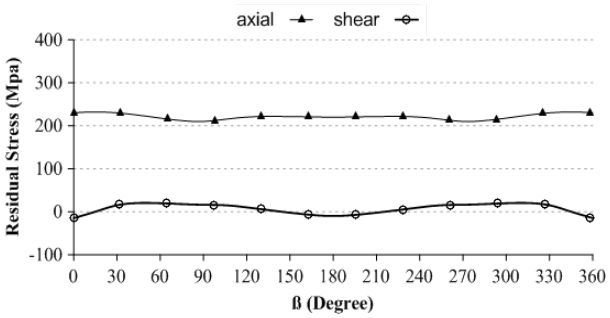

Figure 15. Axial and shear residual stresses in the cross-section of z=50 mm on the outer surface

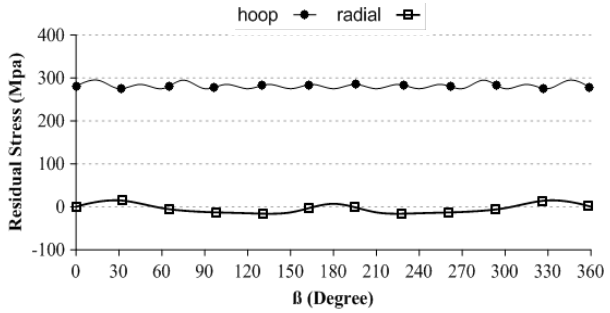

Figure 16. Hoop and radial residual stresses in the cross-section of z=50 mm on the ter surface

The distribution of shear residual stress is negligible because of the symmetric nature of the process and the model, which is the same as the cross-section of z=10 mm.

In the absence of stress concentration on the inner surface at z=50 mm, axial and radial residual stresses have no significant variation in their stress profile.

The profile of axial, shear, hoop and radial residual stresses along the axial direction on the inner and outer surfaces of the workpiece are shown in Figures 17 to 20.

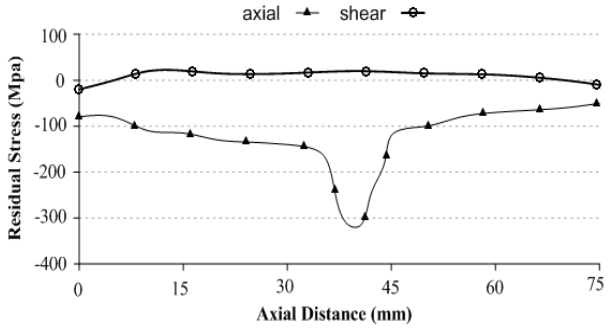

Figure 17. Distribution of axial and shear residual stresses on the inner surface along tube length

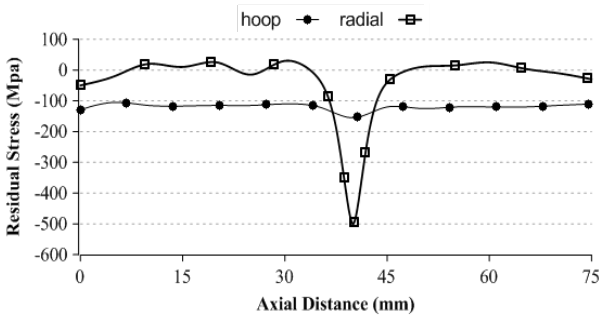

Figure 18. Distribution of hoop and radial residual stresses on the inner surface along tube length

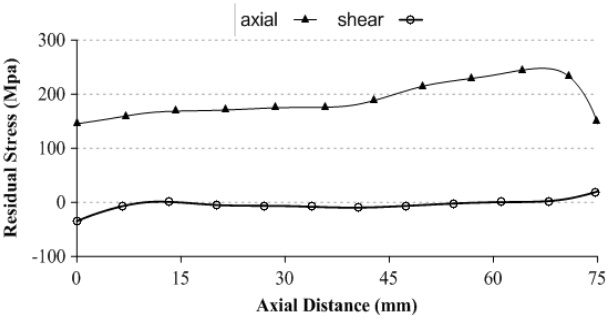

Figure 19. Distribution of axial and shear residual stresses on the outer surface along tube length

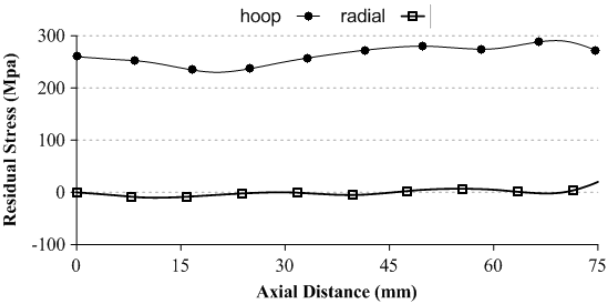

Figure 20. Distribution of hoop and radial residual stresses on the outer surface along tube length

According to Figures 17 to 20, the shear stress on both the surfaces is negligible as expected because of symmetric nature of the workpiece. On the inner surface, axial and radial stresses have a compressive pick due to existence of stress concentration where the groove cross; that is, the profile of stress only passes one groove along length direction.

In the outer surface, the distribution of all these stresses is almost uniform along the tube length except at its ends [10]. In comparison with the axial and hoop stresses, radial stress on the outer surfaces is small and negligible. This is expected because the hammers are

removed and due to existence of free surfaces, the radial stress is removed as well.

The variation of residual stresses on the outer surface versus the axial feed per stroke of workpiece is shown in Figure 21. It can be seen here that the shear and radial stresses have no sensitivity on axial feed. However, the axial and hoop stresses intensify with an increase in the axial feed per stroke. Indeed, the variation in axial feed has a considerable effect on the axial residual stresses. This is due to the fact that more axial feed rate causes more material flow in the axial direction.

Most of the previous studies conducted on the RFP have used axisymmetric models where the rotational feed of the workpiece as a parameter cannot be simulated. Rotational speed is applied as the angle of rotation per blow with a constant axial feed of workpiece in this study. Variations of the residual stresses on the outer surface of the tube with respect to the rotational speed are presented in Figure 22; where the shear and radial residual stresses are constant and an increase in the rotational speed from 26.67 RPM to 53.33 RPM, would gradually amplify the axial and hoop residual stresses on the outer surface of the tube. This process is symmetric in nature, so that the variation of rotational speed does not affect the magnitudes of residual stresses.

The residual stresses versus friction coefficients between the die-tube and the mandrel-tube are presented in Figure 23. In this study, the friction coefficients between the die-tube and the mandrel-tube are considered equal. The magnitude of friction coefficient varies between 0.1 to 0.3. It is evident that in cold metal forming process the friction force has no significant effect as much as hot metal forming. Therefore, the residual stresses vary only slightly with the deviation of friction coefficient.

Mises residual stress distributions on the inner surface for an arbitrary cross-section, where helical grooves are located, are also assessed versus various reductions' percentages. It is obvious that the maximum Mises residual stress must occur at the head part of outstanding grooves which is specified for one groove on the mandrel cross-section, marked with "A" in Figure 24.

The Mises residual stress distribution on the inner surface of the mentioned cross-section for different reduction percentages are shown in Figure 25.

The maximum Misses residual stress increases as the tube reduction is increased. This matter is due to the fact that reduction enhancement causes an increase of forging load and material flow especially at radial direction.

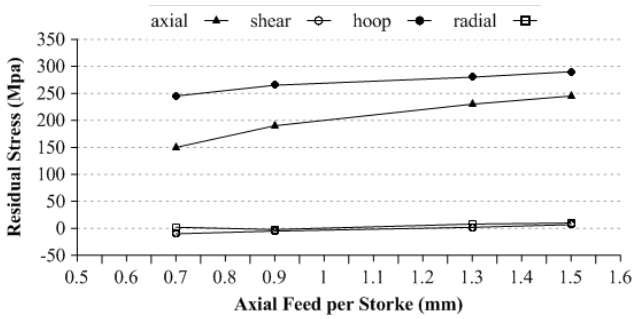

Figure 21. Variation of residual stresses with the axial feed per stroke on the outer surface of the forged tube

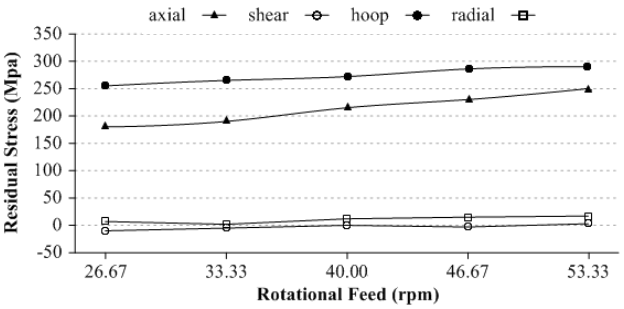

Figure 22. Variation of residual stresses with the rotational feed per stroke on the outer surface of the forged tube

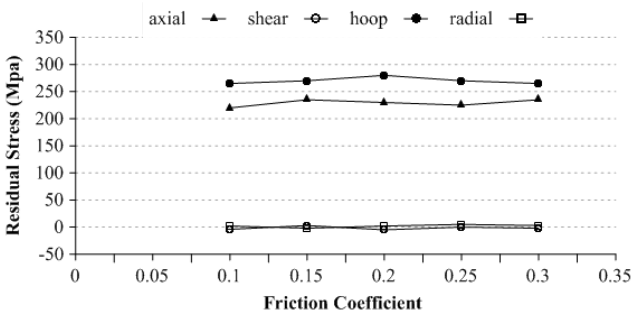

Figure 23. Variation of residual stresseswith friction coefficient between die-tube and mandrel-tube on the outer surface of the forged tube

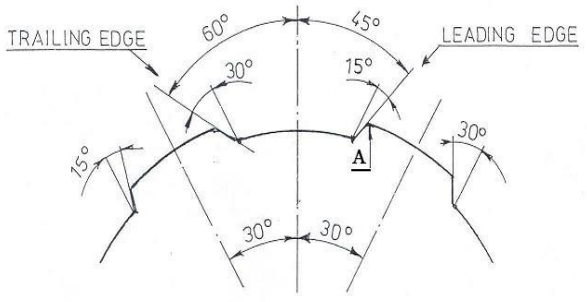

Figure 24. Specified point 'A' that is Head part of outstanding groove

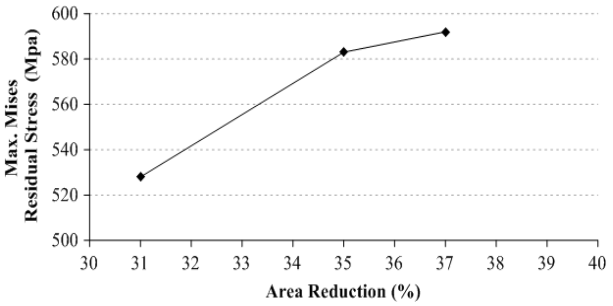

Figure 25. Variation of maximum Mises residual stress versus tube area reduction on the inner surface

6. CONCLUSIONS

In this study, for the first time the residual stresses of a short hollow tube with six internal helical grooves and two steps along its length, in a cold radial forging process are assessed through a 3D FEM. The numerical model is validated with the results of the experimental measurements, the slab method and the upper bound method predictions. It is observed that there is a good agreement between the results of the FEM and other methods. In addition to residual stress distributions, the effective parameters like the axial feed per stroke, rotational feed per stroke, friction coefficient and percentage of reduction on the residual stresses are assessed. It can be concluded from the results that generally the residual stress's distributions on the inner surface in the most points are compressive which prevent the crack propagation. The residual stress distributions on the outer surface are tensile. Therefore, the heat treatment of the cylinder outer surface is essential to improve the fatigue life. The shear residual stress is small and negligible, which is due to the fact that this problem is symmetric and the axial, radial, and hoop directions are the principle stress axis. The radial residual stresses appear due to existence of stress concentration and they are removed on other surfaces. By changing the rotational speed and axial feed, it is found that shear and radial residual stresses have no sensitivity. However, the axial and hoop residual stresses intensify with an increase in the rotational speed and axial feed per stroke where the rotational speed has less sensitivity. Friction coefficient is not effective on residual stresses. Furthermore, by increasing the percentage of area reduction of the tube, the maximum Mises residual stress increases. Therefore, the most important parameters affecting the residual stresses distribution are the workpiece motion and tube area reduction.

7. REFERENCES

1. Farrahi, G., Smith, D., Zhu, W. and McMahon, C., "Influence of residual stress on fatigue life of hot forged and shot blasted steel components", ***International Journal of Engineering-Transactions B: Applications***, Vol. 15, No. 1, (2001), 79-86.
2. Noyan, I. and Cohen, J., "Residual stresses in materials", ***American Scientist***, Vol., No., (1991), 142-153.
3. Lahoti, G. and Altan, R., *Analysis and optimization of the radial forging process for manufacturing gun barrels*. 1974, DTIC Document.
4. Lahoti, G. and Altan, T., "Analysis of the radial forging process for manufacturing rods and tubes", ***Journal of Manufacturing Science and Engineering***, Vol. 98, No. 1, (1976), 265-271.
5. Lahoti, G., Dembowski, P. and Altan, T., "Radial forging of tubes and rods with compound-angle dies", ***Proceeding of NAMRC-IV, May***, (1976), 17-19.
6. Domblesky, J.P., Shivpuri, R. and Painter, B., "Application of the finite-element method to the radial forging of large diameter tubes", ***Journal of materials processing technology***, Vol. 49, No. 1, (1995), 57-74.
7. Jang, D. and Liou, J., "Study of stress development in axi-symmetric products processed by radial forging using a 3-d non-linear finite-element method", ***Journal of materials processing technology***, Vol. 74, No. 1, (1998), 74-82.
8. Subramanian, T., Venkateshwar, R., Lahoti, G. and Lee, F., "Experimental and computer modeling of die cavity fill in radial forging of riflings", ***Materials and Processing Congresses, 1978-1979***, (1980), 185-203.
9. Yang, S., "Research into gfm forging machine", ***J. Mater. Process. Technol***, Vol. 28, (1991), 307-319.
10. Ameli, A. and Movahhedy, M., "A parametric study on residual stresses and forging load in cold radial forging process", ***The International Journal of Advanced Manufacturing Technology***, Vol. 33, No. 1-2, (2007), 7-17.
11. Ghaei, A., Taheri, A.K. and Movahhedy, M., "A new upper bound solution for analysis of the radial forging process", ***International Journal of Mechanical Sciences***, Vol. 48, No. 11, (2006), 1264-1272.
12. Ghaei, A. and Movahhedy, M.R., "Die design for the radial forging process using 3d fem", ***Journal of materials processing technology***, Vol. 182, No. 1, (2007), 534-539.
13. Mahmoudi, A., Hosseinzadeh, A. and Jooya, M., "Plasticity effect on residual stresses measurement using contour method", ***International Journal of Engineering***, Vol. 26, No. 10, (2013).
14. Uhlig, A., "Investigation of the motions and the forces in radial swaging", ***German, Doctoral dissertation, Technical University Hannover***, (1964).
15. Oh, S.-I. and Altan, T., "Metal forming and the finite-element method, Oxford university press, (1989).
16. Altan, T., Oh, S.-I. and Gegel, G., "Metal forming fundamentals and applications", ***American Society for Metals, 1983***, (1983).
17. Khayatzadeh, S., Poursina, M. and Golestanian, H., "A simulation of hollow and solid products in multi-pass hot radial forging using 3d-fem method", ***International Journal of Material Forming***, Vol. 1, No. 1, (2008), 371-374.

Prediction of Residual Stresses for a Hollow Product in Cold Radial Forging Process

M. Poursina [a], H. Alijani Renani[a], B. Ghasemi [b]

[a] *Department of Mechanical Engineering, University of Isfahan, Iran*
[b] *Department of Mechanical Engineering, Khomeini shahr Azad University, Iran*

P A P E R I N F O

Paper history:
Received 02 April 2015
Received in revised form 23 May 2015
Accepted 30 July 2015

Keywords:
Cold Radial Forging
Residual Stress
Mandrel Forging
3-D FEM.

چکیده

آهنگری شعاعی یک فرآیند آهنگری قالب باز است که برای کاهش قطر محورها، لوله‌ها، محورهای پله‌ای و همچنین برای ساخت پروفیل‌های داخلی مانند خان لوله‌های تفنگ استفاده می‌شود. آهنگری شعاعی لوله‌ها معمولا به وسیله یک سنبه به منظور ساخت پروفیل داخلی و یا تغییر اندازه قطر داخلی انجام می‌شود. اکثر تحقیقات انجام شده در زمینه فرآیند آهنگری شعاعی از مدل‌های متقارن محوری استفاده کرده‌اند. در این پژوهش، تنش‌های پسماند یک لوله کوتاه توخالی در فرآیند آهنگری شعاعی سرد با استفاده از شبیه‌سازی اجزاء محدود سه بعدی، مورد بررسی قرار می‌گیرد. در این مطالعه برای اولین بار از سنبه‌ای شامل شش شیار مارپیچ و دو پله در امتداد طول آن استفاده شده است. قطعه کار به صورت یک ماده الاستیک–پلاستیک مدل شده و از نرم‌افزار تجاری اجزاء محدود آباکوس برای شبیه‌سازی فرآیند استفاده شده است. دقت مدل شبیه‌سازی شده به وسیله مقایسه نتایج پیش‌بینی شده آن با آزمایش‌های عملی در دسترس و همچنین روش‌های تختال و کران بالا، اعتبارسنجی می‌شود. تنش‌های پسماند در محصول فرآیند آهنگری شعاعی و تاثیر پارامترهای ساخت بر توزیع تنش مانند حرکت قطعه کار، اصطکاک و درصد کاهش سطح به منظور تعیین پارامترهای بهینه شبیه‌سازی و بهبود شرایط این فرآیند مورد مطالعه قرار می‌گیرد

***doi**: 10.5829/idosi.ije.2015.28.08b.14*

.